

Measurement of type-I ELM pulse propagation in SOL through BES use of MSE diagnostics in JT-60U and impact of ELM on MSE diagnostics

T. Suzuki¹, N. Oyama¹, N. Asakura¹ and T. Fujita¹

¹*Japan Atomic Energy Agency, Naka, Japan*

1. Introduction

Since transient heat and particle loads by type-I ELMs are significantly high for the plasma facing components of the fusion reactor, the propagation of ejected plasma by ELMs (ELM pulse) in scrape-off layer (SOL) is an important issue. Increase in the SOL plasma density due to the ELM pulse has been measured through the increase in beam emission (BE) from heating neutral beam (NB) at various radial locations in the SOL near the equatorial plane, using MSE diagnostics as beam emission spectroscopy (BES) diagnostics in JT-60U [1]. From the temporal delay of the increase of BE as a function of major radius in the SOL, the radial velocity of the ELM pulse propagation has been evaluated. In order to evaluate the propagation velocity accurately, the elimination of the background (BG) light from the BES signal (containing both BE and BG light) is found essential because the delay of the net BE increase by ELM pulse is veiled by the BG light synchronized with ELMs. The intermittent increase in BG light synchronized with ELMs has been observed in MSE channels viewing not only the SOL but also the main plasma in JT-60U. Since this BG light affects the magnetic pitch angle measurement by MSE diagnostics as was reported in JET [2], the impact of the intermittent BG light by ELMs on MSE diagnostics has been numerically investigated in detail. MSE diagnostics can measure ELM pulse propagation in SOL, but on the other hand, BG light by ELMs disturbs MSE diagnostics.

2. Measurement of Type-I ELM Pulse Propagation in SOL Using MSE Diagnostics as BES Diagnostics (MSE/BES)

Propagation of ELM pulse is measured in a type-I ELM My H-mode discharge at $I_p=1.6$ MA and $B_t(0)=4.0$ T ($q_{95}=3.9$) with optimized plasma shape where as many MSE measurement points (including a background channel at ch7) are placed in the SOL as shown in Fig. 1. A two-wavelength detector at ch7 observes not only the BE but also the BG light simultaneously at slightly different wavelength. Figure 2 shows the waveforms of BE (raw and smoothed) as well as BG (smoothed) signal at ch7. Large amplitude oscillation in raw BE signal is not the noise but the

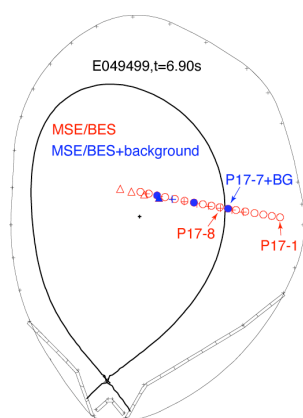


Fig. 1: Last closed flux surface (LCFS) of plasma shown in figure 3, with measurement points of MSE diagnostics (red). The BE and BG signals are simultaneously measured at 3 points indicated by filled circles (blue).

modulation induced by PEM for MSE diagnostics. The smoothed BE signal clearly synchronizes to the D_α emission at the divertor. Relative calibration of BE and BG detectors is performed during a short break of NB during $t \sim 6.88-6.91$ s, where there is no BE so that both of the BE and BG detectors view only the BG light. As seen in Fig. 2, both BE and BG signals agree well with each other during the NB break, indicating waveforms at different wavelength of the BE and BG detectors are similar. Thus, the difference between the BE and BG signals shows the net BE that represents plasma and neutral density in the SOL. The increment of the net BE at ELM is roughly proportional to the plasma density of ELM pulse, since NB power is almost constant.

Although the relative calibration of BE and BG detectors are done using smoothed signals, smoothed signals cannot be used in ELM pulse propagation study since smoothing veils the delay of net BE increase. Instead, we employed conditional average technique in order to eliminate the large oscillation induced by the PEMs. Using 594 ELMs having peak D_α emission larger than 1×10^{20} phs/s/sr/m² for 7 s, the net BE signal has been conditionally averaged with respect to the peak of D_α emission at the divertor. Figure 3(a) shows the comparison of net BE at channels 6 and 7, where ch6 is away from the plasma than ch7 by 62 mm. Clear delay of net BE increase at ch6 than ch7 is observed. If the BG light is not eliminated, no delay between channels 6 and 7 is found (Fig. 3(b)). Figure 4 shows the major radius of MSE measurement points in the SOL as a function of delay with respect to peak of divertor D_α emission.

Using 5 spatial channels located at 0.02-0.3 m outside LCFS, radial velocity of ELM pulse propagation is evaluated to be 0.8-1.8 km/s. A least-mean-squared fitting gives about 1.4 km/s. This result is consistent with measurement using Langmuir probes (1-2.5 km/s) in JT-

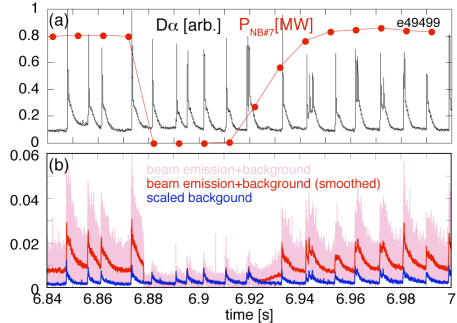


Fig. 2: (a) D_α emission at outer divertor and power of diagnostic NB#7 for MSE. (b) Raw signal (pink) of MSE/BES diagnostics at ch7 viewing outside of plasma and smoothed signal (red) using average of ± 50 ms data. Oscillation at large amplitude in the raw signal is caused by modulation of a pair of PEM devices at 20 kHz and 23 kHz. Smoothed BG signal at ch7 scaled by least-mean-squared fitting to BE signal during $t=6.88-6.91$ s (no beam emission) is indicated in blue.

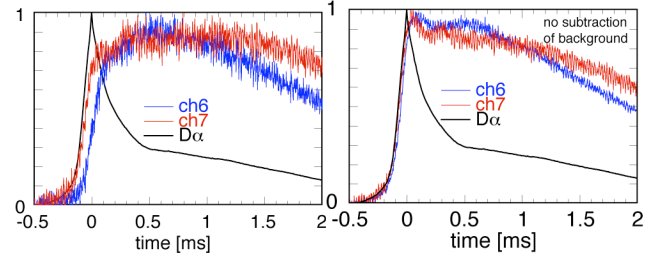


Fig. 3: (a) D_α emission (black) and net beam emission at channels 6 (blue) and 7 (red) conditionally-averaged with respect to the peak of D_α emission over 594 ELMs. All waveforms in this figure are normalized; average of signal during 0.4-0.5 s before the peak of D_α emission is set to zero, and the maximum of each signal is set to unity in this figure. (b) the same as Fig. 3 (a), but background emission is not subtracted from the beam emission.

60U [3]. If BG emission is not eliminated, no clear delay evaluated, since BG emission observed simultaneously in all channels veils the delay in net BE increase.

3. Impact of ELM on MSE Diagnostics

Most MSE diagnostics employ a pair of photo-elastic modulators (PEMs) in measuring polarization angle γ of Stark-splitting σ (or π) component of D_α emission from NB particle (velocity v_b) in magnetic field B , which is perpendicular (or parallel) to $v_b \times B$ Lorentz field. Two PEMs having individual axis directions combined with a linear polarizer temporally modulate polarization state of the incident light at two individual frequencies (f_1 and f_2). The spectrum amplitudes at the frequencies give $\gamma_{\text{PEM}} = -0.5 \tan^{-1} (S_{2f1}/S_{2f2}) + 22.5^\circ$, where S_{2f1} and S_{2f2} are the spectral amplitudes at frequencies $2f_1$ and $2f_2$, respectively. When intermittent BG light by ELMs mixes with the PEM modulation, broadband spectrum of the impulse-like BG light disturbs the spectral amplitudes, even if the BG light is not polarized.

Numerical simulations are carried out using dual-phase software lock-in amplifiers in detecting the spectral amplitudes in the mixed waveforms of PEM modulated BE and BG light by repetitive ELM pulses. The BG light by ELMs is characterized by its peak intensity normalized by intensity of BE (X_{ELM}), ELM frequency (f_{ELM}) and decay time constant (τ_{ELM}). The software lock-in amplifier is designed to simulate the hardware lock-in amplifier used in JT-60U (Stanford Research Systems SR830). Low-pass filter (LPF) in the lock-in amplifier characterizes the temporal response of the MSE diagnostics. The lock-in amplifier has 4 stages of RC-type LPF with its time constant per single stage τ_{LPF} , so that apparent time constant is about $4\tau_{\text{LPF}}$.

Figure 5 shows the waveforms of the simulations for different ELM frequencies $f_{\text{ELM}}=20$ Hz and 100 Hz at $X_{\text{ELM}}=1$, $\tau_{\text{ELM}}=2$ ms, $\tau_{\text{LPF}}=3$ ms and $\gamma=20^\circ$. In case of $f_{\text{ELM}}=20$ Hz, an error in γ_{PEM} induced by single ELM

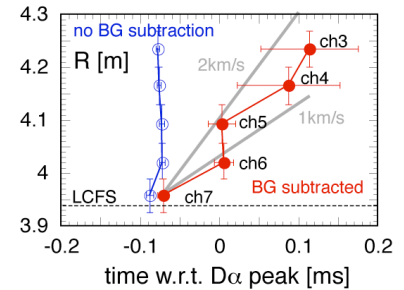


Fig. 4: Major radius of measurement point as a function of time when beam emission signal becomes 0.4 of total beam emission increment (0.4 in Fig. 3). Time is indicated with respect to D_α peak. Filled circles corresponds to net beam emission after background subtraction (Fig. 3(a)), while open circles to no background subtraction (Fig. 3(b)).

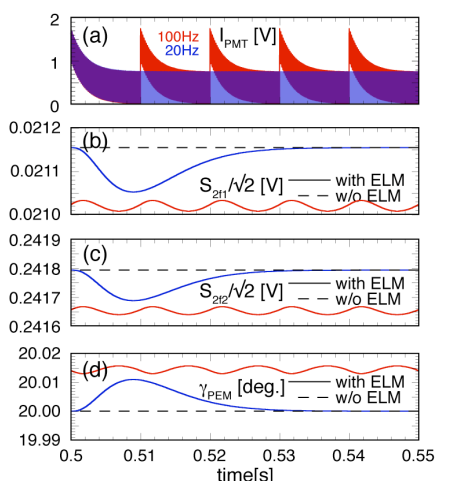


Fig. 5: Waveforms of simulation for $f_{\text{ELM}}=20$ Hz (blue) and 100 Hz (red) at $X_{\text{ELM}}=1$, $\tau_{\text{ELM}}=2$ ms, $\tau_{\text{LPF}}=3$ ms and polarization angle of incident light $\gamma=20^\circ$. (a) PMT signal, (b) $2f_1=40$ kHz amplitude, (c) $2f_2=46$ kHz amplitude, (d) polarization angle measured using PEMs. Dashed lines in (b)-(d) are the corresponding values without ELMs.

increases just after the ELM and then decreases to zero, both in a time scale of about $4\tau_{\text{LPF}}$. However, in case of $f_{\text{ELM}}=100$ Hz, the error induced by each ELM piles up and remains between subsequent ELMs.

Figure 6 shows the error induced by ELMs in systematic scans of the simulation parameters. The average error increases with increase in X_{ELM} and f_{ELM} . However, the maximum error does not depend on f_{ELM} in lower f_{ELM} regime than a critical frequency $f_{\text{ELM,cr}} \sim 1/(4\tau_{\text{LPF}}) = 83$ Hz. This is because the maximum error is mainly determined by the peak of error just after the ELM, as shown in $f_{\text{ELM}}=20$ Hz case in Fig. 5. The error almost does not depend on τ_{ELM} , because the error is mainly caused by broadband frequency spectrum induced at the impulse-like increase in BG emission. In case of the τ_{LPF} scan, the maximum error increases with decrease in τ_{LPF} below a critical time scale, because the spectral power of BG light by ELMs concentrate in a short period just after the ELM. The critical time scale is $1/4f_{\text{ELM}}=2.5$ ms for $f_{\text{ELM}}=100$ Hz in the scan in Fig. 6(d). In a longer τ_{LPF} than the critical time scale, error induced by ELMs piles up and the maximum and minimum errors converge to the average value, as is similar to explanation in f_{ELM} scan. Thus, the behaviour of error induced by ELM changes with f_{ELM} and the choice of τ_{LPF} in lock-in amplifier. These simulations indicate that careful treatment of error induced by ELMs is necessary for MSE diagnostics observing large background light compared to beam emission. The background level of the JT-60U MSE diagnostics is lower than that of the JET MSE [2]. X_{ELM} is roughly estimated to be about 0.1 in the ELMy H-mode discharge in section 2 of this paper ($f_{\text{ELM}} \sim 100$ Hz). Corresponding error for $\tau_{\text{LPF}}=3$ ms is $\sim 0.002^\circ$ which is sufficiently smaller than error in calibration ($\sim 0.1\text{--}0.2^\circ$).

This work was supported by KAKENHI 20760586.

References

- [1] T. Suzuki, *et al.*, Rev. Sci. Instrum. **81**, 043502 (2010).
- [2] R. Coelho, *et al.*, Rev. Sci. Instrum. **80**, 063504 (2009).
- [3] N. Asakura, *et al.*, J. Nucl. Mater. **337-339**, 712 (2005).

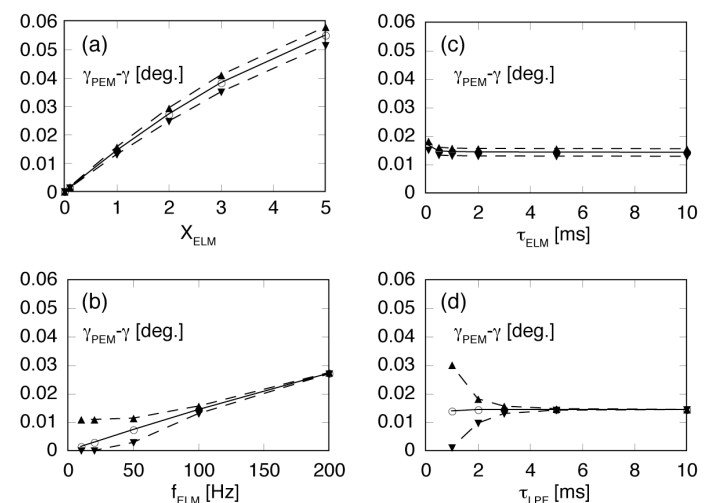


Fig. 6: Dependence of error induced by ELMs on various simulation parameters (a) X_{ELM} , (b) f_{ELM} , (c) τ_{ELM} and (d) τ_{LPF} . Solid curves show the temporal average of error for 1s period, and the dashed curves show the maximum (with upward triangles) and the minimum (with downward triangles). Polarization angle of incident light is $\gamma=20^\circ$ and base simulation parameters are $X_{\text{ELM}}=1$, $f_{\text{ELM}}=100$ Hz, $\tau_{\text{ELM}}=2$ ms, $\tau_{\text{LPF}}=3$ ms, unless the parameter is the scanned parameter.